PAPER

Check for updates

Synthesis-temperature-regulated multi-enzyme-mimicking activities of ceria nanozymes†

Xiaoli Liu,‡[a] Jiangjiexing Wu, [iD] ‡*[b] Quanyi Liu,[cd] Anqi Lin, [iD] [b] Sirong Li,[b]
Yihong Zhang,[b] Quan Wang,[b] Tong Li,[b] Xueying An,[ef] Zijun Zhou,[b] Ming Yang*[ag]
and Hui Wei [iD] *[bh]

Ceria (CeO$_2$) nanozymes have drawn much attention in recent years due to their unique physiochemical properties and excellent biocompatibility. It is therefore very important to establish a simple and robust guideline to regulate CeO$_2$ with desired multi-enzyme-mimicking activities that are ideal for practical bioapplications. In this work, the multi-enzyme-mimicking activities of CeO$_2$ were regulated in a facile manner by a wet-chemical method with different synthesis temperatures. Interestingly, a distinct response in multi-enzyme-mimicking activities of CeO$_2$ was observed towards different synthesis temperatures. And the regulation was ascribed to the comprehensive effect of the oxygen species, size, and self-restoring abilities of CeO$_2$. This study demonstrates that high-performance CeO$_2$ can be rationally designed by a specific synthesis temperature, and the guidelines from radar chart analysis established here can advance the biomedical applications of ceria-based nanozymes.

Introduction

Nanozymes, or nanomaterial-based enzyme mimics, are attractive not only for their stability and eco-efficiency but also for their unique nanomaterial physicochemical properties.[1–10] In particular, benefiting from rich redox properties and surface chemistry,

[a] *School of Pharmacy, State Key Laboratory of Southwestern Chinese Medicine Resources, Chengdu University of Traditional Chinese Medicine, Chengdu, Sichuan 611137, China. E-mail: mingyang26@126.com*

[b] *Department of Biomedical Engineering, College of Engineering and Applied Sciences, Nanjing National Laboratory of Microstructures, Jiangsu Key Laboratory of Artificial Functional Materials, Chemistry and Biomedicine Innovation Center (ChemBIC), Nanjing University, Nanjing, Jiangsu 210023, China. E-mail: wujiangjiexing2007@126.com, weihui@nju.edu.cn*

[c] *State Key Laboratory of Electroanalytical Chemistry, Changchun Institute of Applied Chemistry, Chinese Academy of Sciences, Changchun, Jilin 130022, China*

[d] *University of Science and Technology of China, Hefei, Anhui 230026, China*

[e] *State Key Laboratory of Pharmaceutical Biotechnology and Jiangsu Key Laboratory of Molecular Medicine, School of Medicine, Nanjing University, Nanjing, Jiangsu 210023, China*

[f] *Department of Sports Medicine and Adult Reconstructive Surgery, Nanjing Drum Tower Hospital, The Affiliated Hospital of Nanjing University Medical School, Nanjing, Jiangsu 210093, China*

[g] *Key Laboratory of Modern preparation of Traditional Chinese Medicine, Ministry of Education, Jiangxi University of Chinese Medicine, Nanchang, Jiangxi 330000, China*

[h] *State Key Laboratory of Analytical Chemistry for Life Science and State Key Laboratory of Coordination Chemistry, School of Chemistry and Chemical Engineering, Nanjing University, Nanjing, Jiangsu 210023, China*

† Electronic supplementary information (ESI) available. See DOI: 10.1039/d1tb00964h

‡ These authors contributed equally to this work.

some nanozymes are endowed with more than one type of enzyme-mimicking activity.[11–15] Such multi-enzyme-mimicking activities are demonstrated to act as self-cascade reactors and have been found to be helpful for eliminating or producing multiple reactive oxygen species (ROS) in different therapies, unlike natural enzymes, which have a sole activity against various ROS.[16,17] Among the developed nanozymes with multi-enzyme-mimicking activities, ceria nanozyme (CeO$_2$), a typical and widely-explored nanozyme, can mimic superoxide dismutase (SOD), catalase (CAT), oxidase (OXD), peroxidase (POD), alkaline phosphatase (ALP) enzymes, *etc.*[18–24] The diverse range of enzyme-mimicking activities has led to the use of ceria nanozyme in various biomedical applications, from *in vitro* diagnosis (such as in the detection of glucose, glutathione, and ATP) to *in vivo* therapies (such as ischemic stroke protection, septicaemia, and tumour therapeutics).[25–35]

Despite the significant progress that has been achieved for the ceria nanozyme, few studies have focused on regulation accompanied with analysis for multi-enzyme-mimicking activities, so that an effective guideline for further applications remains lacking. On the one hand, until now, for most CeO$_2$ nanozymes, strategies such as doping, surface modification, and complex formation have been proved to regulate single-type enzyme-mimicking catalytic properties.[36–42] On the other hand, different catalytic reaction processes and uncertain regulation mechanisms make it difficult to regulate multi-enzyme-mimicking activities by a universal strategy. For instance, both SOD- and CAT-mimicking activities have been helpful for eliminating ROS, but the regulation of the Ce^{3+}

fraction has the opposite effect for simultaneously adjusting of SOD- and CAT-mimicking activities.[20,21] It is of note that the role of CeO_2 nanozymes can be switched by changing the pH of the microenvironment, such as being a pro-oxidant under acidic conditions (for peroxidase- and oxidase-like activity) and an anti-oxidant under neutral or alkaline conditions (for SOD- and CAT-like activity).[43] Nevertheless, it is worth noting that pH-dependent regulation of the multi-enzyme-mimicking activities does not provide the most beneficial window for practical applications. For example, the retained SOD-mimicking activity under acidic conditions, although poor, will still weaken the pro-oxidant effect and may even cause potential side effects. On account of the above dilemma, the development of effective strategies and robust guidelines is highly desirable to achieve precise and simultaneous control over the multi-enzyme-mimicking activities of the ceria nanozyme.

In this work, a facile synthetic strategy combined with radar chart analysis has been developed to regulate the multi-enzyme-mimicking activities of CeO_2 with precise and simultaneous adjustment for biomedical applications (Fig. 1). The route involves fine control over the crystal size, the ratio of surface oxygen (O_β) to lattice oxygen (O_α), and surface potential, through a wet-chemical method with different synthesis temperatures (from $-30\ ^\circ C$ to $90\ ^\circ C$). As a result, the multi-enzyme-mimicking activities of CeO_2 are effectively modulated. The observed regulation of each enzyme-mimicking activity under different synthesis temperatures is summarized and established as a guideline. Finally, the identified guideline is found to be helpful for advancing further biomedical applications of ceria-based nanozymes.

Experimental

Preparation of CeO_2

CeO_2 was synthesized following our previously published procedure.[37] First, 504 mg $Ce(NO_3)_3 \cdot 6H_2O$ was dissolved in 20 mL of ethylene glycol aqueous solution (v/v = 1:1) under vigorous stirring, and then the mixture was placed under different temperatures (-30, 0, 30, 60, and $90\ ^\circ C$) with further vigorous stirring. After 5 min, 4 mL of aqueous ammonia (28–30%) were quickly injected into the mixture. With continuous stirring for 3 h, the products were subsequently collected by centrifugation, washed with excess deionized water, and modified with citric acid to adjust the pH to about 7.0. Finally, the CeO_2 solutions were stored or dried by lyophilization for further applications. Note, the as-prepared CeO_2 samples prepared at different temperatures are denoted as Ceria_-30, Ceria_0, Ceria_30, Ceria_60, and Ceria_90.

SOD-mimicking activity of CeO_2

According to the protocol of the SOD assay kit (Dojindo, Japan), the CeO_2 nanozyme (20 μL, 1 mg mL^{-1}) was first mixed with 200 μL of a 2-(4-iodophenyl)-3-(4-nitrophenyl)-5-(2,4-disulfophenyl)-2H tetrazolium sodium salt working solution in respective microplate wells. Then, 20 μL of the enzyme working solution was added to each mixture, gently mixed, and incubated for 30 min at $37\ ^\circ C$. Later, the absorbance at 450 nm was measured using a microplate reader.

CAT-mimicking activity of CeO_2

First, dopamine (0.1 mL, 1 mg mL^{-1}) and H_2O_2 (5 μL, 20 mM) were added to 50 mM Tris–HCl buffer (pH = 8.5) containing the CeO_2 nanozyme. Detection solutions were incubated in a low-oxygen environment at $37\ ^\circ C$ by anaerobic gas generating bag. After 30 min, all samples were measured at 405 nm using a microplate reader.

1,1-Diphenyl-2-picrylhydrazyl (DPPH)-scavenging activity of CeO_2

The CeO_2 nanozyme (0.08 mL, 1 mg mL^{-1}) was mixed with DPPH (0.5 mL, 0.05 mg mL^{-1}) in methanol solution and 0.42 mL methanol, respectively. After incubation in the dark at $37\ ^\circ C$ for 24 h, the absorbance of the mixture at 517 nm was recorded using a microplate reader.

POD-mimicking activity of CeO_2

In a typical POD-mimicking activity measurement, the CeO_2 nanozymes (0.02 mL, 2 mg mL^{-1}), H_2O_2 (0.1 mL, 1 M), and TMB (100 μL, 20 mM) were sequentially added to 1.78 mL of 200 mM acetate buffer solution (pH = 4.5). After 4 min, the absorbance of the reaction solution at 652 nm was measured using a UV-vis-spectrometer.

OXD-mimicking activity of CeO_2

In a typical OXD-mimicking activity measurement, the CeO_2 nanozymes (0.025 mL, 2 mg mL^{-1}), and TMB (0.1 mL, 20 mM) were sequentially added into 1.875 mL of a 200 mM acetate buffer solution (pH = 4.5). After 24 h, the reaction solutions were measured at 652 nm using a UV-vis-spectrometer.

ALP-mimicking activity of CeO_2

In a typical ALP-mimicking activity measurement, the CeO_2 nanozymes (0.1 mL, 2 mg mL^{-1}) and p-NPP (0.1 mL, 0.05 mg mL^{-1}) were added to 0.8 mL Tris buffer solutions (pH = 10.0) in sequence. After incubation at $37\ ^\circ C$ for 1 h, the reaction solutions were recorded at 405 nm using a microplate reader.
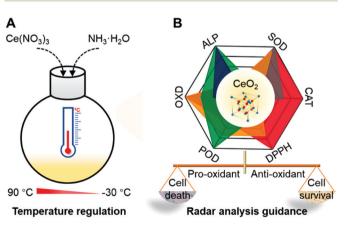

Fig. 1 Synthesis of ceria nanozymes *via* temperature regulation to optimize the multi-enzyme-mimicking activity for biomedical applications.

This journal is © The Royal Society of Chemistry 2021

J. Mater. Chem. B, 2021, **9**, 7238–7245 | **7239**

Results and discussion

Synthesis and characterization of CeO_2

The CeO_2 nanozymes were prepared using a wet-chemical method. To investigate the effect of different synthesis temperatures on the structures and physiochemical properties of CeO_2, five different temperatures ($-30\ ^\circ$C, $0\ ^\circ$C, $30\ ^\circ$C, $60\ ^\circ$C, and $90\ ^\circ$C) were chosen here to synthesize the CeO_2 (Fig. 2A). An ethylene glycol/water (1 : 1) antifreeze solution and an aqueous ammonia solution (28%) with low melting points were utilized to prepare the CeO_2 samples under different temperatures, especially for low-temperature environments below $0\ ^\circ$C.

As shown in Fig. 2B, all obtained CeO_2 samples were mono-disperse due to their negative zeta potentials (about -30 mV) with a crystal size smaller than 10 nm (Fig. S1 and Table S1, ESI†). Their highly crystalline nature was confirmed by the high-resolution transmission electron microscope (TEM) images in the insets (Fig. 2B). A comparison between the CeO_2 samples synthesized under different temperatures showed that the size of CeO_2 decreased as the synthesis temperature was decreased. Further analysis, by counting about 65 particles, illustrated that the average size of Ceria_90, Ceria_60, Ceria_30, Ceria_0, and Ceria_-30 was 4.2 ± 0.7 nm,

3.7 ± 0.6 nm, 3.1 ± 0.6 nm, 2.6 ± 0.3 nm, and 2.5 ± 0.5 nm, respectively (Fig. 2C). The X-ray diffraction (XRD) patterns of the different CeO_2 samples shown in Fig. 2D matched well with the standard cubic fluorite structure of ceria, confirming the identical structures of the CeO_2 samples synthesized under different temperatures. Notably, the full width at half maximum values for CeO_2 synthesized at low temperatures were significantly larger than that at high temperature, which indicated that a smaller size was easy to acquire at low temperatures, matching with the TEM results.[44]

The X-ray photoelectron spectroscopy (XPS) results in Fig. S2 (ESI†) confirmed the presence of both Ce and O elements in all synthesized CeO_2. Further XPS analyses for the Ce 3d core level in Fig. S3 (ESI†) provided the oxidation state of Ce on the surface. The results in Fig. S3 and Table S1 (ESI†) showed that both Ce^{3+} and Ce^{4+} existed in all the obtained CeO_2 samples with Ce^{4+} being dominant. And the fraction of Ce^{3+} depicted "volcanic" type tendency with Ceria_-30, Ceria_0, Ceria_30, Ceria_60, and Ceria_90 (Fig. S4, ESI†). In the collection of O 1s core level spectra for all synthesized CeO_2 samples (Fig. S5, ESI†), a broad signal between 527.5 and 537.5 eV was obtained and deconvoluted to analyse the surface oxygen (O_β) and lattice oxygen (O_α) species. A similar "volcanic" tendency with
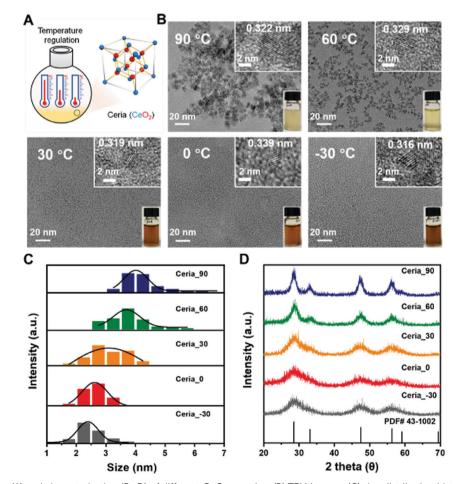

Fig. 2 Synthesis scheme (A) and characterization (B–D) of different CeO_2 samples: (B) TEM images, (C) size distribution histograms of CeO_2 measured from TEM images, and (D) XRD patterns.

7240 | *J. Mater. Chem. B*, 2021, **9**, 7238–7245

This journal is © The Royal Society of Chemistry 2021

Ceria_−30, Ceria_0, Ceria_30, Ceria_60, and Ceria_90 was observed in Fig. S6 (ESI†). Moreover, the specific surface areas (S_{BET}) of all synthesized CeO_2 samples were determined through the N_2 adsorption isotherm, and the S_{BET} value of Ceria_−30, Ceria_0, Ceria_30, Ceria_60, and Ceria_90 was 158.2, 179.8, 192.5, 166.0, and 135.6 m^2 g^{-1}, respectively (Fig. S7, ESI†). Therefore, all the above characterizations indicated that different synthesis temperatures allowed fine regulation of the size, surface potential, Ce^{3+} fractions, O_β fractions, and surface area of the CeO_2 samples. And these factors mentioned above play important roles in most catalytic reactions, and encouraged us to further investigate the multi-enzyme-mimicking activities of Ceria_−30, Ceria_0, Ceria_30, Ceria_60, and Ceria_90.

Multi-enzyme-mimicking activities of CeO2

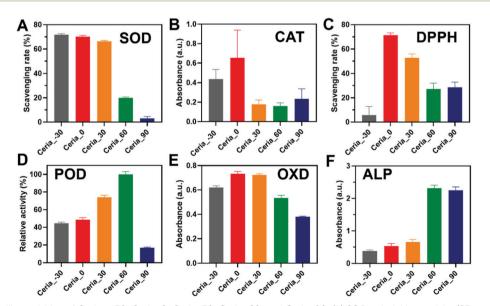Before investigating the multi-enzyme-mimicking activities of CeO_2, the catalytic self-restoring ability of Ceria_−30, Ceria_0, Ceria_30, Ceria_60, and Ceria_90 was assessed through treatment with H_2O_2. As shown in Fig. S8A (ESI†), a red-shift phenomenon in UV-visible light transmittance was first observed for Ceria_−30, Ceria_0, Ceria_30, Ceria_60, and Ceria_90 with H_2O_2 injected for 5 min. In addition, the corresponding solution changed from a faint pale yellow to orange (Fig. S8B, ESI,† red box), indicating the change from Ce^{3+} to Ce^{4+}. Then after 7 days, the colour of all the solutions returned to their original colour (Fig. S8C, ESI,† blue box), and a blue-shift reflecting the change from Ce^{4+} to Ce^{3+} was also detected in the UV-visible light transmittance.[45] This finding illustrated that Ceria_−30, Ceria_0, Ceria_30, Ceria_60, and Ceria_90 possess catalytic self-restoring abilities, guaranteeing the basis for enzyme-mimicking catalytic abilities.

Motivated by the above results, diverse enzyme-mimicking activities (Fig. S9, ESI†) of Ceria_−30, Ceria_0, Ceria_30, Ceria_60, and Ceria_90 were performed and compared under the same conditions to study the effect of the different synthesis temperatures on the multi-enzyme-mimicking activities of the ceria nanozyme. As shown in Fig. 3A and Fig. S10 (ESI†), the SOD-mimicking activity of Ceria_−30, Ceria_0, Ceria_30, Ceria_60, and Ceria_90 was studied using a SOD assay kit. The SOD-mimicking activities of Ceria_−30, Ceria_0, and Ceria_30 were similar, better than those of Ceria_60 and Ceria_90. Remarkably, a more than twenty-fold increase in the SOD-mimicking activity was observed by changing the synthesis temperature from 90 °C to −30 °C.

The CAT-mimicking activity of the ceria nanozyme was studied by monitoring the absorbance changes at 405 nm of oxidized dopamine in a hypoxic environment, as the O_2 produced by decomposing H_2O_2 could oxidize the dopamine. As shown in Fig. 3B, the CAT-mimicking activity of Ceria_−30, Ceria_0, Ceria_30, Ceria_60, and Ceria_90 presented a "volcanic" type plot tendency, with Ceria_0 showing the best CAT-mimicking activity. Interestingly, a similar "volcanic" tendency was observed with the DPPH-scavenging activity of the ceria nanozymes (Fig. 3C and Fig. S11, ESI†). Here, the DPPH eliminating efficiency of Ceria_0 was twelve times of that of Ceria_−30.

The POD- and OXD-mimicking activities of Ceria_−30, Ceria_0, Ceria_30, Ceria_60, and Ceria_90 were monitored using TMB as the model substrate.[46] The ceria nanozyme catalysed the oxidation of TMB, and subsequently generated a blue product with an absorption feature peak at 652 nm (Fig. S12, ESI†). As shown in Fig. 3D, the POD-mimicking activity was enhanced with an increase in the synthesis temperature from −30 °C to 60 °C, before sharply declining at 90 °C. The POD-mimicking activity of Ceria_60 exceeded by about 5 times that of Ceria_90. The enzyme-mimicking activity of two other peroxidase-type enzymes, haloperoxidase (HPO)

Fig. 3 Multi-enzyme-like activities of Ceria_−30, Ceria_0, Ceria_30, Ceria_60, and Ceria_90. (A) SOD-mimicking activity (83 µg mL^{-1} ceria, n = 3), (B) CAT-mimicking activity (20 µg mL^{-1} ceria, n = 4), (C) DPPH-scavenging ability (80 µg mL^{-1} ceria, n = 4), (D) POD-mimicking activity (20 µg mL^{-1} ceria, n = 4), (E) OXD-mimicking activity (25 µg mL^{-1} ceria, n = 4), and (F) ALP-mimicking activity (200 µg mL^{-1} ceria, n = 3).

This journal is © The Royal Society of Chemistry 2021

J. Mater. Chem. B, 2021, **9**, 7238–7245 | **7241**

and glutathione peroxidase (GPx), were also systematically evaluated for the ceria nanozymes. As shown in Fig. S13 and S14 (ESI†), respectively, negligible HPO- and GPx-mimicking activities were observed. For OXD-mimicking activity, the results shown in Fig. 3E depict a similar "volcanic" tendency as that observed in the CAT- and DPPH-scavenging activities.

Besides the redox-type enzyme-mimicking activities mentioned above, ceria nanozyme has also been reported to behave as a hydrolase mimic. To systematically study the ALP-mimicking activity of the ceria nanozyme, *para*-nitrophenyl phosphate (*p*-NPP) was used as the model substrate, and the absorbance at 405 nm of *p*-nitrophenol was monitored. As shown in Fig. 3F, distinct from redox-type enzyme-mimicking activities, the ALP-mimicking activity of ceria nanozyme increased as the synthesis temperature was elevated. Moreover, the ALP-mimicking activities of Ceria_60 and Ceria_90 were comparable, about six times that of Ceria_−30.

These above observations unambiguously demonstrated that the synthesis temperature could regulate the multi-enzyme-mimicking catalytic activities of ceria nanozymes. We subsequently found that the SOD-mimicking, CAT-mimicking, OXD-mimicking, and DPPH-scavenging catalytic activities were well correlated with the ratio of O_β/O_α, while for the POD-mimicking and ALP-mimicking catalytic activities, a negative correlation was displayed with the ratio of O_β/O_α (Fig. S6, ESI†). These results collectively indicated that the oxygen species played a dominant role in the multi-enzyme-mimicking catalytic activities of Ceria_−30, Ceria_0, Ceria_30, Ceria_60, and Ceria_90, which is consistent with previous reports.[37,47,48] It is worth mentioning that there are some rationales underlying the multi-enzyme-mimicking catalytic activities of the ceria nanozymes. For Ceria_90, all the redox-type catalytic activities were low, which can be attributed to the worse catalytic self-restoring ability of Ceria_90 with the large blue shift shown in Fig. S8A (ESI†). Likewise, the

SOD-mimicking activity of the ceria nanozymes was not of a "volcanic" type, and the higher activity of Ceria_−30 over Ceria_0 may come from the smaller size of the Ceria_−30. Taken together, all the results indicated that for the modulation of these multi-enzyme-mimicking activities, the key factor is the oxygen species, and other factors such as crystal size also play certain roles. Therefore, several factors including the crystal size, oxygen species, and self-restoring abilities affected by the different synthesis temperatures have a comprehensive effect on the multi-enzyme-mimicking activities of ceria nanozymes.

Although the multi-enzyme-mimicking activities of Ceria_−30, Ceria_0, Ceria_30, Ceria_60, and Ceria_90 can be regulated by the different synthesis temperatures, different responses exist between Ceria_−30, Ceria_0, Ceria_30, Ceria_60, and Ceria_90. To make it easier for elucidation and analysis, a series of radar charts was drawn based on the results in Fig. 3. As shown in Fig. 4, Ceria_0 has the highest activities in both SOD-mimicking, CAT-mimicking, DPPH-scavenging, and OXD-mimicking. By contrast, the worst activity in SOD-mimicking, CAT-mimicking, DPPH-scavenging, POD-mimicking and OXD-mimicking was found for Ceria_90. According to previous studies,[27,49–53] the SOD-mimicking, CAT-mimicking and DPPH-scavenging activities eliminate the reactive free radicals, thus endowing the ceria nanozymes with anti-oxidant ability. Conversely, POD-mimicking and OXD-mimicking activities show the pro-oxidant property of ceria nanozymes.[36,54–56] Therefore, combining these findings, Ceria_0 with its high SOD-mimicking, CAT-mimicking, and DPPH-scavenging activities would be chosen as an anti-oxidant, rather than Ceria_−30 or Ceria_30. Moreover, compared with Ceria_−30 and Ceria_30, it would be better to select Ceria_60 and Ceria_90 as a pro-oxidant. Based on the above results, the strategy of synthesis temperature-guided regulation and the guidelines developed here will not only enhance the enzyme-mimicking activities of the ceria nanozyme, but also provide a guideline for
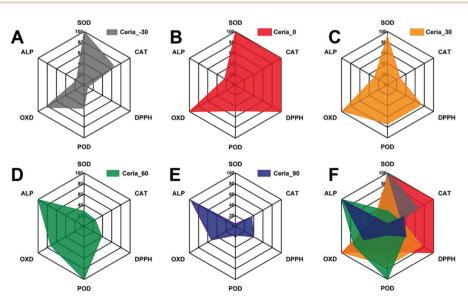

Fig. 4 Radar charts of the multi-enzyme-mimicking activities of (A) Ceria_−30, (B) Ceria_0, (C) Ceria_30, (D) Ceria_60, (E) Ceria_90, and (F) all nanozyme samples combined.

7242 | *J. Mater. Chem. B*, 2021, **9**, 7238–7245

This journal is © The Royal Society of Chemistry 2021

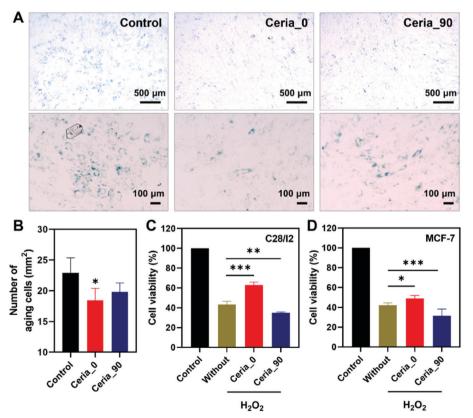rational application of the nanozymes in complex biological systems.

Anti-aging effect of CeO$_2$

Since Ceria_0 possessed excellent anti-oxidant properties, an anti-aging cytoprotection ability was studied here to demonstrate the capability of Ceria_0 for relieving cellular oxidative stress in biological systems. Before investigating the potential biological applications, the biocompatibility of ceria nanozymes was first assessed. As shown in Fig. S15 (ESI†), after incubation with human bone marrow mesenchymal stem cells (hMSCs) for 24 h, at concentrations even up to 200 µg mL^{-1}, the ceria nanozymes showed no cytotoxicity on the hMSCs, indicating their excellent biocompatibility. Subsequently, considering the accumulation of oxidative stress with increasing age,[57,58] the ability of Ceria_0 provide cytoprotection against senescence was investigated by co-incubating with cells. After 7 days of cultivation, compared with the control group, the group treated with the Ceria_0 nanozyme remained spindle cells with a regular shape and a distinct profile, which suggested that the Ceria_0 nanozyme could provide cytoprotection from aging (Fig. S16, ESI†). To quantify the anti-aging effect of the Ceria_0 nanozymes, we used a senescence β-galactosidase staining kit assay. As shown in Fig. 5A, the Ceria_0 nanozyme-treated group showed a significant anti-aging effect, with only 18 aging cells per square millimetre

(Fig. 5B). While for the control group, the galactosidase staining showed that untreated cells were obviously in an aging status with around 23 aging cells per square millimetre. Thus, the significantly decreased number of aging cells showed the excellent anti-aging capability of the Ceria_0 nanozymes, protecting cells from aging-induced oxidative stress. However, when Ceria_90, with a worse activity, was applied, the anti-aging effect was not so obvious and was comparable to control group (Fig. 5B). In addition, to further evaluate the anti-aging effect of the Ceria_0 nanozymes, another typical aging model induced by D-galactose was also studied and a similar result as the natural aging model was obtained (Fig. S17, ESI†). Together, the above results confirmed that the Ceria_0 nanozyme, selected from the developed guidelines, did exhibit an excellent anti-oxidant property and protected cells from aging-induced oxidative damage.

Selective cytoprotection effect of CeO$_2$

To further evaluate the guiding effect of the developed guidelines for biomedical applications, the human normal chondrocyte cell line (C28/I2 cell), which needs to be protected from oxidative stress, and the human breast cancer cell line (Michigan cancer foundation-7, MCF-7 cell), which needs to be killed, were chosen here. As shown in Fig. 5C, when being exposed to H$_2$O$_2$, the C28/I2 cell viability decreased to 40%, in comparison with that of the control group; also, the treatment of Ceria_0 would alleviate

Fig. 5 Cytoprotection under different treatments. (A) Photos of hMSC staining with X-gal (blue or green area). (B) Quantitative statistical results of aging cells from (A) (*n* = 5). * means *P* < 0.05 *vs.* the control group. (C and D) Cell viability for human normal chondrocyte cell line (C28/I2 cell) and human breast cancer cell line (Michigan cancer foundation-7, MCF-7 cell) (*n* = 5). * means *P* < 0.05 *vs.* the H$_2$O$_2$ group. ** means *P* < 0.01 *vs.* the H$_2$O$_2$ group. *** means *P* < 0.001 *vs.* the H$_2$O$_2$ group.

This journal is © The Royal Society of Chemistry 2021

J. Mater. Chem. B, 2021, **9**, 7238–7245 | **7243**

H_2O_2-induced oxidative stress, with the cell viability being restored to 70%. However, for Ceria_90, the weaker CAT-mimicking and DPPH-scavenging activities could not protect the C28/I2 cell effectively against oxidative stress. The finding here is consistent with the above anti-aging results, confirming the excellent anti-oxidant properties of the Ceria_0 nanozyme as guided by the radar charts.

By contrast, in the MCF-7 cells, which needs to be killed, Ceria_90 with a pro-antioxidant activity was capable of further reducing the cell viability (Fig. 5D). Notably, even though with OXD- and POD-mimicking activities to act as a pro-antioxidant, Ceria_0 could not kill the MCF-7 cells as effectively as Ceria_90. This worse effect may be attributed to the retained anti-oxidant (such as SOD-mimicking) activity under the acidic pH of the MCF-7 cell environment. The results here not only highlighted the importance of the simultaneous control and analysis of multi-enzyme-mimicking activities, but also confirmed the directing effect of the developed radar-map guidelines for biomedical applications. With this meaningful strategy, a suitable ceria nanozyme could be selected to obtain the most effective window for advancing further biomedical applications.

Conclusions

In summary, we have developed an effective and convenient strategy to modulate the multi-enzyme-mimicking activities of ceria nanozymes by changing the synthesis temperature from −30 to 90 °C. Further characterization and multi-enzyme-mimicking activity studies allowed us to elucidate oxygen species as the key factor and other synergistic cofactors (such as the size and self-restoring ability) in regulating the multi-enzyme-mimicking activities of ceria nanozymes. Moreover, a detailed radar analysis of the multi-enzyme-mimicking activities of the ceria nanozymes may guide the rational development and selection of a desired nanozyme. Finally, we demonstrated that Ceria_0, with the best anti-oxidant activity as guided by the radar analysis, did exhibit significant cytoprotection from aging- and H_2O_2-induced oxidative damage. However, for killing cancer cells, Ceria_90 rather than Ceria_0 would be a better choice. Thus, this work provides not only a facile strategy to simultaneously modulate the multi-enzyme-mimicking activity of nanozymes, but also an effective guideline to advance the development of ceria nanozymes and their further biomedical applications in biological systems.

Author contributions

X. L. and J. W. performed the experiments and wrote the paper. Q. L., A. L., S. L., Y. Z., Q. W., T. L., X. A., and Z. Z. directed and performed the analysis of experiments. Q. L. and Y. Z. revised the paper. H. W., J. W. and M. Y. contributed to supervision and directed the project. All authors reviewed the paper.

Conflicts of interest

There are no conflicts to declare.

Acknowledgements

References

1 J. Wu, X. Wang, Q. Wang, Z. Lou, S. Li, Y. Zhu, L. Qin and H. Wei, *Chem. Soc. Rev.*, 2019, **48**, 1004–1076.
2 H. Wei and E. Wang, *Chem. Soc. Rev.*, 2013, **42**, 6060–6093.
3 D. Jiang, D. Ni, Z. T. Rosenkrans, P. Huang, X. Yan and W. Cai, *Chem. Soc. Rev.*, 2019, **48**, 3683–3704.
4 Y. Huang, J. Ren and X. Qu, *Chem. Rev.*, 2019, **119**, 4357–4412.
5 L. Gao, J. Zhuang, L. Nie, J. Zhang, Y. Zhang, N. Gu, T. Wang, J. Feng, D. Yang, S. Perrett and X. Yan, *Nat. Nanotechnol.*, 2007, **2**, 577–583.
6 F. Natalio, R. Andre, A. F. Hartog, B. Stoll, K. P. Jochum, R. Wever and W. Tremel, *Nat. Nanotechnol.*, 2012, **7**, 530–535.
7 R. Fang and J. Liu, *J. Mater. Chem. B*, 2020, **8**, 7135–7142.
8 X. Hu, T. Huang, H. Liao, L. Hu and M. Wang, *J. Mater. Chem. B*, 2020, **8**, 4428–4433.
9 L. Huang, J. Chen, L. Gan, J. Wang and S. Dong, *Sci. Adv.*, 2019, **5**, eaav5490.
10 Z. Wang, R. Zhang, X. Yan and K. Fan, *Mater. Today*, 2020, **41**, 81–119.
11 B. Liu and J. Liu, *Nano Res.*, 2017, **10**, 1125–1148.
12 X. Jiang, P. Gray, M. Patel, J. Zheng and J. J. Yin, *J. Mater. Chem. B*, 2020, **8**, 1191–1201.
13 Y. Li, H. Zhou, T. Li, X. Jian, Z. Gao and Y. Y. Song, *J. Mater. Chem. B*, 2021, **9**, 2016–2024.
14 P. Zhang, D. Sun, A. Cho, S. Weon, S. Lee, J. Lee, J. W. Han, D. P. Kim and W. Choi, *Nat. Commun.*, 2019, **10**, 940.
15 Q. Wang, J. Chen, H. Zhang, W. Wu, Z. Zhang and S. Dong, *Nanoscale*, 2018, **10**, 19140–19146.
16 Q. Zhang, H. Tao, Y. Lin, Y. Hu, H. An, D. Zhang, S. Feng, H. Hu, R. Wang, X. Li and J. Zhang, *Biomaterials*, 2016, **105**, 206–221.
17 T. Kang, Y. G. Kim, D. Kim and T. Hyeon, *Coord. Chem. Rev.*, 2020, **403**, 213092.
18 A. Asati, S. Santra, C. Kaittanis, S. Nath and J. M. Perez, *Angew. Chem., Int. Ed.*, 2009, **48**, 2308–2312.
19 X. Jiao, H. Song, H. Zhao, W. Bai, L. Zhang and Y. Lv, *Anal. Methods*, 2012, **4**, 3261–3267.
20 T. Pirmohamed, J. M. Dowding, S. Singh, B. Wasserman, E. Heckert, A. S. Karakoti, J. E. S. King, S. Seal and W. T. Self, *Chem. Commun.*, 2010, **46**, 2736–2738.

7244 | *J. Mater. Chem. B*, 2021, **9**, 7238–7245

This journal is © The Royal Society of Chemistry 2021

21 E. G. Heckert, A. S. Karakoti, S. Seal and W. T. Self, *Biomaterials*, 2008, **29**, 2705–2709.

22 T. Yao, Z. Tian, Y. Zhang and Y. Qu, *ACS Appl. Mater. Interfaces*, 2019, **11**, 195–201.

23 Z. Tian, T. Yao, C. Qu, S. Zhang, X. Li and Y. Qu, *Nano Lett.*, 2019, **19**, 8270–8277.

24 K. Korschelt, R. Schwidetzky, F. Pfitzner, J. Strugatchi, C. Schilling, M. von der Au, K. Kirchhoff, M. Panthofer, I. Lieberwirth, M. N. Tahir, C. Hess, B. Meermann and W. Tremel, *Nanoscale*, 2018, **10**, 13074–13082.

25 B. Liu, Z. Sun, P.-J. J. Huang and J. Liu, *J. Am. Chem. Soc.*, 2015, **137**, 1290–1295.

26 C. Xu and X. Qu, *NPG Asia Mater.*, 2014, **6**, e90.

27 C. K. Kim, T. Kim, I. Y. Choi, M. Soh, D. Kim, Y. J. Kim, H. Jang, H. S. Yang, J. Y. Kim, H. K. Park, S. P. Park, S. Park, T. Yu, B. W. Yoon, S. H. Lee and T. Hyeon, *Angew. Chem., Int. Ed.*, 2012, **51**, 11039–11043.

28 D. Jampaiah, T. Srinivasa Reddy, V. E. Coyle, A. Nafady and S. K. Bhargava, *J. Mater. Chem. B*, 2017, **5**, 720–730.

29 H. Song, K. Ye, Y. Peng, L. Wang and X. Niu, *J. Mater. Chem. B*, 2019, **7**, 5834–5841.

30 X. Chen, H. Xing, Z. Zhou, Y. Hao, X. Zhang, F. Qi, J. Zhao, L. Gao and X. Wang, *J. Mater. Chem. B*, 2021, **9**, 1491–1502.

31 B. Bhushan and P. Gopinath, *J. Mater. Chem. B*, 2015, **3**, 4843–4852.

32 F. Li, Y. Qiu, F. Xia, H. Sun, H. Liao, A. Xie, J. Lee, P. Lin, M. Wei, Y. Shao, B. Yang, Q. Weng and D. Ling, *Nano Today*, 2020, **35**, 100925.

33 P. Lin, M. Cao, F. Xia, H. Liao, H. Sun, Q. Wang, J. Lee, Y. Zhou, Y. Guan, C. Zhang, Z. Xu, F. Li, J.-F. Wei and D. Ling, *Adv. Sci.*, 2021, **8**, 2004115.

34 T. Huang, X. Hu, M. Wang, Y. Wu, L. Hu and Z. Xia, *Chem. Commun.*, 2021, **57**, 3054–3057.

35 H. Liao, Y. Liu, M. Chen, M. Wang, H. Yuan and L. Hu, *Microchim. Acta*, 2019, **186**, 274.

36 H. J. Cheng, S. C. Lin, F. Muhammad, Y. W. Lin and H. Wei, *ACS Sens.*, 2016, **1**, 1336–1343.

37 W. Guo, M. Zhang, Z. Lou, M. Zhou, P. Wang and H. Wei, *ChemCatChem*, 2019, **11**, 737–743.

38 H. Frerichs, E. Pütz, F. Pfitzner, T. Reich, A. Gazanis, M. Panthöfer, J. Hartmann, O. Jegel, R. Heermann and W. Tremel, *Nanoscale*, 2020, **12**, 21344–21358.

39 Y. Wang, T. Liu and J. Liu, *ACS Appl. Nano Mater.*, 2020, **3**, 842–849.

40 X. Zhao, S. Li, X. Yu, R. Gang and H. Wang, *Nanoscale*, 2020, **12**, 21440–21446.

41 M. Zhu, Y. Wen, S. Song, A. Zheng, J. Li, W. Sun, Y. Dai, K. Yin and L. Sun, *Nanoscale*, 2020, **12**, 19104–19111.

42 A. Gupta, T. S. Sakthivel, C. J. Neal, S. Koul, S. Singh, A. Kushima and S. Seal, *Biomater. Sci.*, 2019, **7**, 3051–3061.

43 Z. Tian, H. Liu, Z. Guo, W. Gou, Z. Liang, Y. Qu, L. Han and L. Liu, *Small*, 2020, **16**, 2004654.

44 V. Uvarov and I. Popov, *Mater. Charact.*, 2013, **85**, 111–123.

45 S. S. Lee, W. Song, M. Cho, H. L. Puppala, P. Nguyen, H. Zhu, L. Segatori and V. L. Colvin, *ACS Nano*, 2013, **7**, 9693–9703.

46 B. Jiang, D. Duan, L. Gao, M. Zhou, K. Fan, Y. Tang, J. Xi, Y. Bi, Z. Tong, G. F. Gao, N. Xie, A. Tang, G. Nie, M. Liang and X. Yan, *Nat. Protoc.*, 2018, **13**, 1506–1520.

47 F. Esch, S. Fabris, L. Zhou, T. Montini, C. Africh, P. Fornasiero, G. Comelli and R. Rosei, *Science*, 2005, **309**, 752–755.

48 A. A. Vernekar, T. Das and G. Mugesh, *Angew. Chem., Int. Ed.*, 2016, **55**, 1412–1416.

49 J. M. Dowding, T. Dosani, A. Kumar, S. Seal and W. T. Self, *Chem. Commun.*, 2012, **48**, 4896–4898.

50 M. Li, P. Shi, C. Xu, J. Ren and X. Qu, *Chem. Sci.*, 2013, **4**, 2536–2542.

51 G. Wang, J. Zhang, X. He, Z. Zhang and Y. Zhao, *Chin. J. Chem.*, 2017, **35**, 791–800.

52 S. Singh, *Biointerphases*, 2016, **11**, 04B202.

53 I. Celardo, M. De Nicola, C. Mandoli, J. Z. Pedersen, E. Traversa and L. Ghibelli, *ACS Nano*, 2011, **5**, 4537–4549.

54 L. Jiang, S. Fernandez-Garcia, M. Tinoco, Z. Yan, Q. Xue, G. Blanco, J. J. Calvino, A. B. Hungria and X. Chen, *ACS Appl. Mater. Interfaces*, 2017, **9**, 18595–18608.

55 X. Jiao, W. Liu, D. Wu, W. Liu and H. Song, *Anal. Methods*, 2018, **10**, 76–83.

56 Z. Tian, J. Li, Z. Zhang, W. Gao, X. Zhou and Y. Qu, *Biomaterials*, 2015, **59**, 116–124.

57 T. Finkel and N. J. Holbrook, *Nature*, 2000, **408**, 239–247.

58 Y. Zhang, Z. Wang, X. Li, L. Wang, M. Yin, L. Wang, N. Chen, C. Fan and H. Song, *Adv. Mater.*, 2016, **28**, 1387–1393.

This journal is © The Royal Society of Chemistry 2021

J. Mater. Chem. B, 2021, **9**, 7238–7245 | **7245**